GONGFA LI*,**,***, DU JIANG**,***#, YING SUN**, GUOZHANG JIANG**,****, BO TAO**

LIFE PREDICTION MECHANISM OF LADLE COMPOSITE STRUCTURE BODY BASED ON SIMULATION TECHNOLOGY

Ladle plays an important role in the metallurgical industry whose maintenance directly affects the production efficiency of enterprises. In view of the problems such as low maintenance efficiency and untimely maintenance in the current ladle passive maintenance scheme, the life prediction mechanism for ladle composite structures is established which bases on the stress analysis of steel shell and ladle lining in the production process, combining conventional fatigue analysis and extended fracture theory. The mechanism is accurate and effective according to the simulation results. Through which, the useful life of steel shell can be accurately predicted by detecting the crack length of it. Due to the large number of factors affecting the life of the lining of the ladle, it is difficult to accurately predict the life of the ladle lining, so a forecasting mean based on the thermal shock method is proposed to predict the service life of the ladle lining in this paper. The life prediction mechanism can provide data support and theoretical guidance for the active maintenance of the ladle, which is the prerequisite for scientifically formulating ladle initiative maintenance program.

Keyword: Ladle life prediction, Initiative maintenance, Crack propagation, Thermal shock method

1. Introduction

Ladles play a role in transporting high-temperature liquid steel in steel production. Extending the service life of the ladle can not only save the production cost, but also reduce the erosion of molten steel on the refractories of the ladle and thus improve the quality of molten steel. Because many factors affect the ladle's life and the technical standards of ladle are not uniform, there are few active maintenance plans for ladle. So the service life of the ladle may be greatly improved by actively and effectively maintaining the operation.

About the longevity technology of ladle, researchers have made significant study. In actual production, the ladle is always subjected to the weight and thermal shock of the molten steel. Therefore, by studying the stress variation and the factors affecting the life of the steel ladle, it is beneficial to the maintenance and maintenance of the ladle. Since the 1970s, the rapid development of the refining technology outside the furnace and the requirements for molten steel quality have become increasingly demanding. Research on lining refractory materials has also received extensive attention. The characteristics of the refractory material not only affect the life of the ladle but also affect the industrial production efficiency. V.V. Slovikovskii [1] analyzed the performance of the cast ladle lining, using high-temperature adhesive as the lining refractories, making the ladle life expectancy increased by 30%-50%. V.A. Kononov et al. [2] studied the high temperature resistant mullite-high silica material and used it as the working lining for ladle thermal insulation and life analysis. The results show that the lining can not only achieve better thermal insulation effect, and can extend the service life of cast ladle. Gongfa Li [3-6] proposed a new type of steel ladle with nano-insulating material lining for the simple lining structure of traditional ladle. The temperature field of the new ladle with nano-insulating material lining was adopted by finite element technology in which the stress field was analyzed and studied. By studying the temperature field and stress field of the new ladle under different working conditions, it was found that the new ladle with nano-liner material had more advantages in thermal insulation performance and ladle life than the traditional ladle. At present, the research on longevity technology of ladle is mainly focused on the research of ladle refractories, improvement of process and maintenance of high temperature equipment [7-10]. However, these methods all passively prolong the life of the ladle, and there is no active prediction mechanism in the maintenance of the later stage. Borges et al. [11] studied the wear mechanism of refractories whose results are of great significance for the analysis of the wear and performance evaluation of ladle. Zhou et al. [12] analyzed the temperature field and stress field

*   THE STATE KEY LABORATORY OF REFRACTORIES AND METALLURGY, WUHAN UNIVERSITY OF SCIENCE AND TECHNOLOGY, WUHAN 430081, CHINA
**   WUHAN UNIVERSITY OF SCIENCE AND TECHNOLOGY, KEY LABORATORY OF METALLURGICAL EQUIPMENT AND CONTROL TECHNOLOGY OF MINISTRY OF EDUCATION, WUHAN 430081, CHINA
***   WUHAN UNIVERSITY OF SCIENCE AND TECHNOLOGY, RESEARCH CENTER FOR BIOMIMETIC ROBOT AND INTELLIGENT MEASUREMENT AND CONTROL, WUHAN 430081, CHINA
****   WUHAN UNIVERSITY OF SCIENCE AND TECHNOLOGY, THE RESEARCH INSTITUTE OF 3D PRINTING AND INTELLIGENT MANUFACTURING ENGINEERING, WUHAN 430081, CHINA

Corresponding author: jiangdu@wust.edu.cn

1556

of the continuous casting tundish cover plate, and analyzed the fatigue life of the critical point using fatigue damage mechanics and modified SN curve. In which, a new fatigue life prediction method was proposed. This method is advantageous for effective monitoring of fatigue cracks in high temperature equipment.

The research on the structure optimization of the ladle and the lining material has greatly extended the service life of the ladle. At the same time, the ladle maintenance is also an important factor affecting the ladle life. Therefore, the study of the ladle's late-term maintenance has the effect of improving the service life of the ladle. This paper will analyze and calculate the ladle shell and liner life of ladle in actual production in combination with specific production conditions, and establish a life prediction mechanism to provide an important theoretical basis for the active maintenance mechanism of ladle.

2. Stress field model of steel shell and ladle lining

The object of this study was the 200/300 t ladle model, as shown in Fig. 1. The slag line working layer in the lining is mainly made of magnesia carbonaceous lining brick. The working layer of the package bottom and the package wall is mainly made of aluminum-magnesium carbonaceous lining brick [13], [14]. The high-aluminum lining brick is mainly used for the bottom layer and the permanent layer of the package wall.
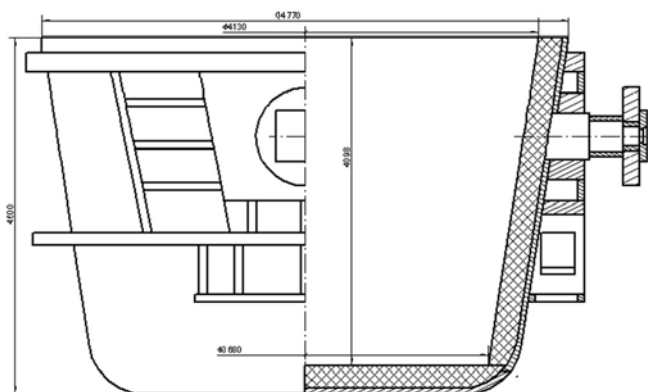

Fig. 1. 200/300 t ladle structure body

Fig. 2 shows the finite element model used in numerical simulation. The finite element model uses automatic meshing, there are 34660 total finite element models, and there are 9668 nodes. The element type is selected according to the calculation. When calculating the temperature field, the selected element type Eight-node thermal entity unit (Solid70) provided for the software. At the same time, in combination with the specific working conditions of the ladle, a heat transfer model of the ladle is established, as shown in Fig. 3.

At simulating the temperature field and stress field of the ladle, the physical property parameters of the material will directly affect the accuracy of the calculation results of the ladle temperature field and stress field. In the calculation of finite element temperature field and stress field, the physicochemi-
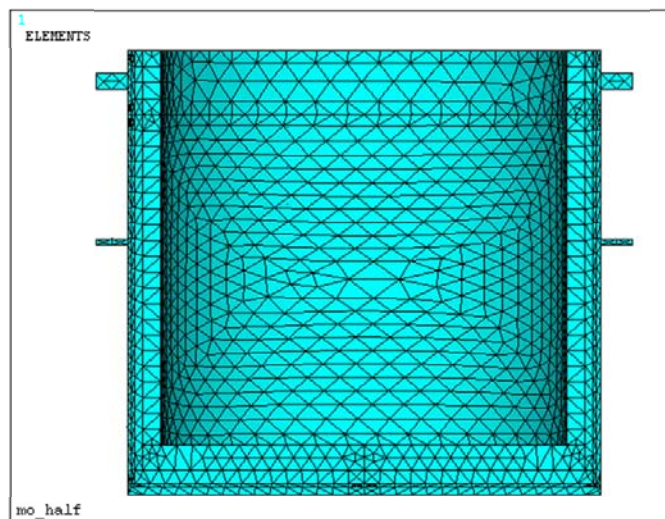

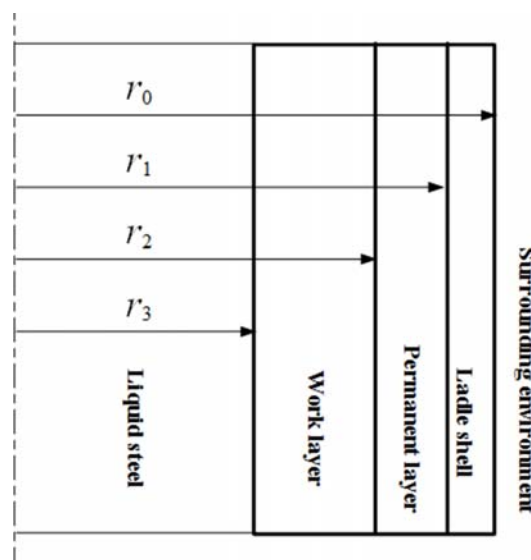Fig. 2. 3D finite element model

Fig. 3. Heat transfer model

cal parameters involved include the material density, thermal conductivity, specific heat, elastic modulus and Poisson's ratio.

The physical parameters used in this study were obtained by consulting the relevant literature. The parameter values are given in Tab. 1-3 [14].

TABLE 1

Thermal conductivity values of ladle bottom and wall refractory

Temperature (C°)	Temperature (C°)			
Thermal conductivity (w/m k)	20	400	800	1200
Working layer (aluminum magnesium carbonaceous)	1.15	—	—	—
Permanent layer (micro expansion high aluminum)	0.5	—	—	—
Slag layer (magnesium carbon)	2.35	2.1	1.75	1.55
Ladle shell	50	39	30	18

TABLE 2

Specific heat capacity of ladle bottom and wall refractories

Specific Heat Capacity (J/kg k) \ Temperature (C°)	Temperature (C°)			
	20	400	800	1200
Working layer (aluminum magnesium carbonaceous)	800	900	1020	1200
Permanent layer (micro expansion high aluminum)	610	750	1175	1320
Slag layer (magnesium carbon)	1080	—	—	—
Ladle shell	400	420	510	600

TABLE 3

Physical parameters values of ladle bottom and wall refractories

Refractory material \ Physical parameters	Coefficient of expansion ($\alpha \times 10^{-6}$ K^{-1})	Density Kg/mm^{-3}	Elastic Modulus (MPa)	Poisson's ratio
Working layer (aluminum magnesium carbonaceous)	8.5	2.95e-6	6300	0.21
Permanent layer (micro expansion high aluminum)	5.8	2.8 e-6	5700	0.21
Slag layer (magnesium carbon)	15	2.9 e-6	8000	0.21
Ladle shell	13	7.8 e-6	175000	0.3

In general, the natural convection coefficient of air and steel cladding is 5 to 10 W/(m²·K), and the more accurate formula is Eq. (1):

$$h = 1.826 \left[\frac{T_s}{T_s - T_a} \right]^{1/3} \qquad (1)$$

In which, h is convective heat transfer coefficient, T_s is steel shell temperature, T_a is the temperature of the surrounding air.

The ability of an object to radiate heat depends on the temperature of the object. Since the ladle temperature of the studied ladle is generally around 170°C to 310°C, the radiant heat conversion can be simplified to the form of convection heat transfer in order to save computing resources. The equivalent convective heat transfer coefficient when the radiative heat exchange between the steel cladding and the surrounding is converted into convection heat can be expressed by Eq. (2).

$$h_r = \varepsilon B (T_s^2 - T_a^2)(T_s - T_a) \qquad (2)$$

In which, h_r is equivalent convection heat transfer coefficient, T_s is temperature of the steel cladding, T_a is the temperature of the surrounding air, B is Boltzmann constant, ε is emissivity.

Since the radiation on the surface of the ladle is similar to the radiation heat transfer system with F1/F2 approaching zero, the emissivity factor is 0.8. In which, $B = 5.67e^{-8}$ W/(m²·K^{-4}), $T_s = 525.7$K, $T_a = 303$K, so $h_r = 13.8$ (W/m²·K^{-1}).

After the above calculation, the radiative and convective heat transfer conditions of the steel cladding are preliminarily determined.

When calculating the stress field, the sequential coupling method is adopted, that is, the temperature field of the model is calculated at first, and then the temperature field result is used as the body load calculated by the stress field to calculate the stress field of the ladle composite structure. When dealing with the boundary conditions, it is necessary to constrain the displacement of the nodes in the y-direction on the symmetry plane of the ladle, and set the nodes on the symmetry plane to be symmetrical. The other constraints are determined according to the different states of the ladle. The loads acting on the ladle model include mechanical load and thermal load, and when calculating the ladle stress field, it is calculated separately under the conditions of lifting, trolley or landing. The support of the ladle on the steel water truck, the lifting and the ladle turret is achieved by applying a z-direction elastic boundary constraint on the corresponding node. The calculation results are shown in Tab. 4.

TABLE 4

Equivalent stress of ladle lining and outer casing under different working conditions

Working conditions	Equivalent stress range of the lining	Equivalent stress range of the outer casing
Under lifting	2.5 MPa~45.0 MPa	2.0 MPa~238.0 MPa
On the trolley	2.3 MPa~44.1 MPa	0.2 MPa~222.0 MPa
Landing	3.9 MPa~37.4 MPa	0.4 MPa~244.3 MPa

In the lift state, the maximum stress appears on the intermediate band on the symmetry plane of the model. On the trolley, the maximum stress of the equivalent stress of the refractory lining appears at the bottom of the slag line on the hot surface of the lining; the maximum stress of the equivalent stress of the steel cladding occurs at the joint of the root of the ladle and the ladle barrel, especially at the ends of the pedestal. In the ground state, the equivalent stress of the refractory lining is between them. The maximum stress appears at the bottom of the slag line on the hot surface of the lining and the maximum stress of the steel cladding appears at the center of the bottom of the package where the bottom support structure of the ladle is not considered. The area of contact with the ground is much larger than the actual situation, and the actual stress at the bottom of the ladle is larger than the calculated value here.

3. Life prediction of steel shell

3.1. Structural Analysis of Steel Shell

In material mechanics, the conditions under which the strength of a component is designed and analyzed are as follows:

For brittle materials: $\sigma \leq [\sigma] = \dfrac{\sigma_b}{n_b}$ (3)

1558

For plastic materials:
$$\sigma \leq [\sigma] = \frac{\sigma_r}{n_r} \qquad (4)$$

In which, σ is the working stress calculated based on the load, $[\sigma]$ is the allowable stress. σ_b, σ_s and σ_r are the ultimate strength, yield limit, and long-lasting limit of the same material. n_b, n_s, n_r are the safety factors of σ_b, σ_s, σ_r.

In terms of strength design, there are the following basic understandings:

(1) The working stress on the member at the time of fracture is relatively low, generally not exceeding the yield limit of the material, and sometimes less than the allowable stress. Even though the member is made of plastic material, brittle fracture may occur for "low stress brittle fracture".

(2) Low-stress brittle fracture is often caused by the presence of a crack source with a length of 0.1-10 mm on the internal surface of the component. The existence of such macro cracks is due to defects in the material smelting process such as various welding defects, scratches, pits, cuts, or corrosion and fatigue during use.

(3) Low-stress brittle fractures of low- and moderate-strength steels generally occur at lower temperatures, and brittle fractures of high-strength steels do not change with temperature.

Although the traditional design method considers the stress concentration factor, the research object is treated as a uniform and continuous object without considering that any material or stressed component inevitably has a certain defect or crack. It is due to the existence of such a crack. The component also suffered a fracture under lower stress. As severe accidents continue to occur, people gradually realize that the traditional strength theory is incomplete [15,16]. Therefore, on the basis of summarizing the fracture accidents, we have found a way to discuss fracture failure from the mechanical point of view, namely the fracture mechanics method. The research object of fracture mechanics is a cracked object, which provides a theoretical basis for correctly considering the influence of the defect on the strength of the component. In this paper, the ladle life prediction is based on fracture mechanics theory.

First of all, fatigue life calculations are required for three locations of the maximum stress points at the base of the new steel cladding trunnion, ladle seat and ladle shell.

According to the stress results calculated by the finite element method, the stress concentration factor is taken into consideration, and the stress of each part is less than the yield limit of the material, and the high-cycle fatigue safety factor method is used for checking [16].

$$n_\sigma = \frac{\sigma_{-1}}{K_{\sigma_D} \times \sigma_a + \psi_\sigma \times \sigma_m} \geq [n] \qquad (5)$$

In which, σ_D is the part fatigue limit when the stress ratio is R. σ_m – Average stress, ψ_a – Average stress conversion factor, σ_a – Stress amplitude. K_{σ_D} – Coefficient of fatigue reduction of parts under symmetric cycle.

1) Checking the root of the steel shell trunnion

Fig. 4 shows the minimum equivalent stress cloud of the 8472 node of the trunnion root, corresponding to the state of the ladle when it lands.
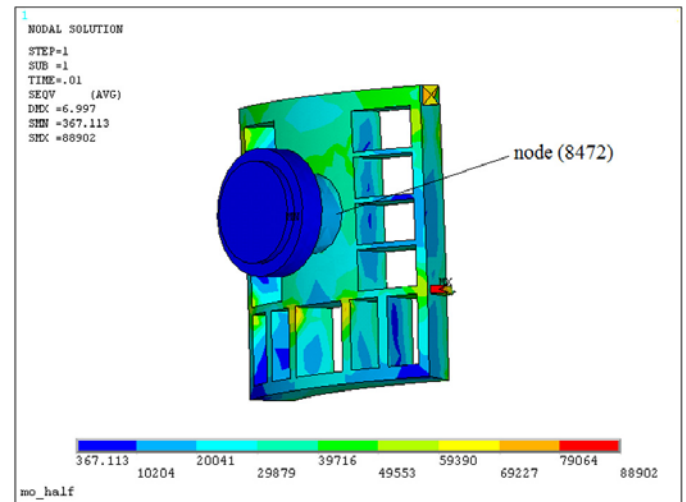

Fig. 4. Equivalent stress cloud diagram of the trunnion of the ladle when landing

According to Fig. 4 and related calculations $\sigma_{max} = 159.39$ MPa, $\sigma_{min} = 13.03$ MPa, $\sigma_m = 86.21$ MPa, $\sigma_a = 73.18$ MPa, and $\varepsilon = 0.55$, $\beta = 0.8$, $K_\sigma = 1$, $\psi_\sigma = 0.1$, so $K_{\sigma_D} = 2.07$, $n_\sigma = 1.46$.

2) Checking of ladle seats

Fig. 5 is the minimum equivalent stress cloud diagram for the 6311 node of the ladle seat, which corresponds to the landing state of the ladle.
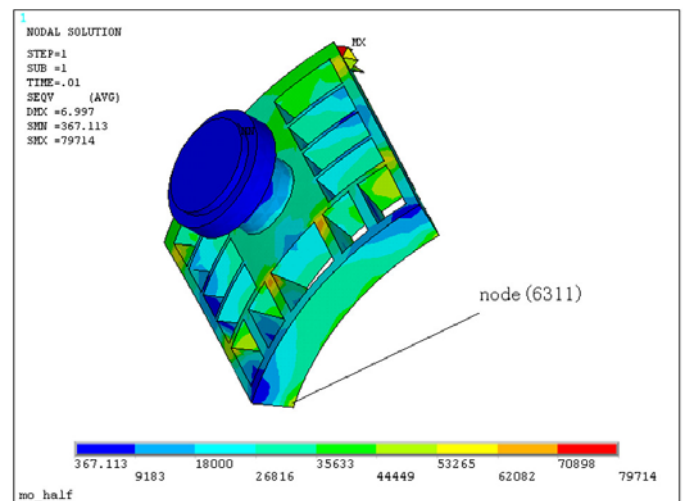

Fig. 5. Equivalent Stress Cloud of Ladle Carriage when Landed

According to Fig. 4 and related calculations $\sigma_{max} = 221.96$ MPa, $\sigma_{min} = 56.29$ MPa, $\sigma_m = 139.13$ MPa, $\sigma_a = 82.84$ MPa. In which $\varepsilon = 0.88$, $\beta = 0.8$, $K_\sigma = 1$, $\psi_\sigma = 0.18$. So, $K_{\sigma_D} = 1.39$, $n_\sigma = 1.25$.

3) Checking the ladle base

Fig. 6 shows the minimum equivalent stress cloud of the ladle base 194, corresponding to the ladle lifting status.
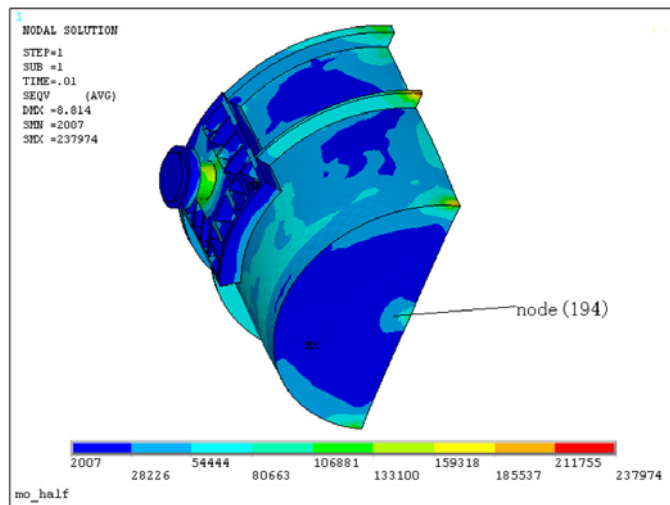

Fig. 6. Equivalent stress cloud diagram of ladle base during lifting

As in Fig. 6, $\sigma_{\max}$ = 244.26 MPa, $\sigma_{\min}$ = 50.72 MPa, σ_m = 147.49 MPa, σ_a = 96.77 MPa. In which ε = 0.88, β = 0.8, K_σ = 1, ψ_σ = 0.05, so K_{σ_D} = 1.39, n_σ = 1.24.

The stress values $\sigma_{\max}$ and $\sigma_{\min}$ at each point in the above three cases are finite element calculation results, and it can be considered that the stress concentration factor has been included, so each K_σ = 1. The selection of the trunnion parameters is based on forging and the rest of the positions are in accordance with the hot-rolled steel plate.

The calculation results show that the safety factors in the above three locations are relatively small, but all are greater than 1. According to design specifications, for a structure such as a ladle, the fatigue factor is greater than two. The above results show that the fatigue life of the steel cladding is not infinite life ($>1 \sim 5\times10^6$). Their lifetime at a safety factor of 2 can be converted according to Eq. (10):

$$N = N_0/K^m \qquad (6)$$

In which, $K = 2/n_\sigma = 2/2.14$; $m = 9$; $N_0 = 10^6$ (Min), so the minimum life is: N = 13537 times.

3.2. Calculation of Extended Life of Ladle

Fatigue fracture is a major form of failure of welded metal structures. It occurs in components subjected to alternating or fluctuating strains. Generally, the maximum stress corresponding to failure is lower than the tensile strength of the material and even lower than the yield strength of the material [5,10,17,18]. Therefore, the fracture is often low without obvious plastic deformation. Stress fracture. According to statistics, the failure of the welded structure due to fatigue cracks accounts for more than 70-80% of the total fracture accidents, and about 50%-90% of the mechanical structures are destroyed by fatigue. The traditional fatigue design theory ignores the cracking of the component itself, but in reality, the presence of cracks in the component will seriously affect the service life of the component.

Metal fatigue failure can be divided into three stages: **1** – microscopic crack propagation stage. Under cyclic loading, due to the non-uniform microstructure of the internal microstructure of the object, microscopic cracks are first formed in some weak parts [19-23]. After that, the cracks expand along the direction of the maximum shear stress that forms an angle of approximately 45° with the principal stress. At this stage, the crack length is approximately within 0.05 mm. If the loading continues, the micro cracks will develop into macroscopic cracks. **2** – Macroscopic crack propagation stage. The crack propagates substantially in a direction perpendicular to the principal stress [24-29]. With the aid of an electron microscope, fatigue strips left over from each stress cycle in this phase can be observed on the fracture surface [30,31]. **3** – instantaneous fracture stage. When the crack expands so that the surviving cross-section of the object is not sufficient to resist the external load, the object will suddenly break under one load. Fig. 7 shows the three stages of crack propagation.
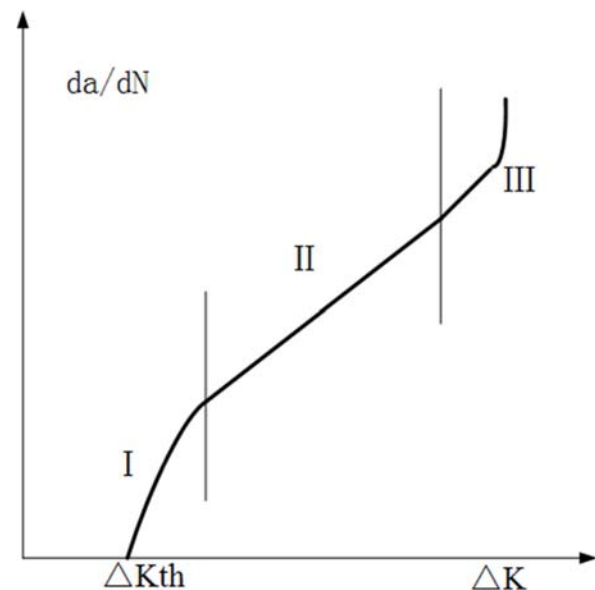

Fig. 7. Three stages of crack propagation

For phase I, the crack no longer propagates when it is reduced to a certain limit value ΔK^{th}, which is called the fatigue threshold value [32]. It is greatly affected by factors such as the average stress, the environment, and the microstructure of the material [26,33-35]. For the crack propagation phase II, P.C. Paris in the United States proposed a formula based on the test results in 1963, which is called the Parisian type:

$$d_a/d_N = C(\Delta K)^m \qquad (7)$$

Where C and m are material constants. For commonly used structural steel aluminum alloys, $m = 2\sim4$.

1560

Parisis is a straight line in the double logarithmic coordinate system, basically in line with the experimental results of phase II. The mechanism of the final phase III of crack propagation is relatively complex, and the proportion of crack growth life is very small so that there are few studies. Taking the ladle bottom as an example, the crack life is calculated and the results are shown in Tab. 5.

TABLE 5

Calculation result of the life of the ladle bottom

Crack propagation threshold	ΔK_{th} (MPa·m$^{0.5}$)	12
	a_{th} (mm)	0.5
a_0 (mm)	ΔK (MPa·m$^{0.5}$)	N (cycle)
0.4	10.70	Infinite life (>10^6)
1	16.92	23042
2	23.93	15781
5	37.83	10949
10	53.50	8977
12	58.61	7593
15	65.52	4119
18	71.78	2231
20	75.66	1432
25	84.59	253
26.7	87.42	11

It can be known from Tab. 5 that the crack length corresponding to the crack propagation threshold value is 0.5 mm, and when the initial crack length is 0.4 mm (<0.5 mm), its lifetime (ie cycle number) is infinity (>106), along with the initial crack With the increase of the length, its life is gradually reduced; when the initial crack length is 15 mm, the crack has developed to a rapid expansion zone, and the corresponding fatigue life is 4119 times; when the initial crack length is 26.7 mm, the corresponding fatigue life is only 11 Second, it can be assumed that the crack propagation has ended and the material will be destroyed.

4. Ladle lining material life prediction

The damage of a solid material is essentially a discrete entity, and its delicate analysis requires that specific micro-defects be treated as discrete disturbances in a continuous medium. Although this theoretical analysis has certain possibilities, it is quite difficult. Therefore, the continuous damage mechanics theory is applied to introduce the damage effect into constitutive equations of continuum mechanics [36], and a continuous damage mechanics model and the corresponding damage evolution equation are established so as to be applied to the treatment of practical problems such as life estimation, safety assessment, and material research [37,38].

According to the continuous damage model, the small voxels in solid materials were studied. It is a material point on the macroscopic level, much smaller than the engineering structure scale, but it is not a micro-structure. Since the parameters such

as mass, strain, stress, and temperature are not evenly continuous in nature, the voxels taken must contain enough microstructure to examine the average behavior and response of each parameter in the body element [39].

The fatigue damage of the refractory lining under thermal stress is closely related to the fatigue behavior of the material under mechanical stress. Thermal fatigue damage is accompanied by the accumulation of microscopic structures and the degeneration of macroscopic physical properties. The propagation of cracks also produces acoustic emission signals. As the number of thermal fatigue increases, the residual compressive strength of the refractory lining will gradually decrease, and the relationship between the number of thermal shocks and the residual strength σ_R after the thermal shock of the refractory lining is expressed as Eq. (8):

$$\sigma_R = A \lg N + B \tag{8}$$

Among them, A and B are material experimental constants.

When the actual stress of the refractory lining reaches its residual strength, the material will break and be damaged [40]. Here, it is assumed that the thermal load is applied alone without chemical corrosion, and that the ladle one-time thermal cycling process is an equal amplitude thermal shock. Taking slag-line magnesia-carbon firebrick as an example, it can be known from the previous section that the maximum equivalent stress of magnesia-carbon firebrick is $\sigma_{max} = 45.0$ MPa, and the compressive strength of magnesia-carbon firebrick is 48 MPa. It is known from literature that magnesium carbon is in the formula of the relationship between the number of thermal shocks and the residual strength of the refractory lining, the constant $A = -1.58$ and $B = 48$ (assuming that the first thermal shock has negligible damage to its compressive strength).

$$N = 10^{\frac{\sigma_R - B}{A}} = 79 \,(\text{Heating times}) \tag{9}$$

It can be seen that when the thermomechanical load is applied alone and the chemical corrosion does not affect the life of the Mg-C refractory lining, the maximum life of the refractory brick is $\sigma_{max} = 45.0$ MPa, and the maximum life can reach 79 times; Under the dual effects of thermomechanical load and chemical corrosion, the service life of the slag layer firebrick is 40 times and the maximum is 46 times. It can be seen that the thermal mechanical load has a great influence on the service life of the slag layer firebrick. Under the double action, the service life under the double action is about half of the lifetime under the effect of the single thermo-mechanical stress. Tab. 6 and Tab. 7 respectively show the maximum thermal stress of the lining of each layer under three supporting conditions, and the life of the ladle lining under the effect of separate thermo-mechanical stress.

From Tab. 7, it can be seen that the damage patterns between the linings of the layers are different. The slag layer has the corrosion and thermal load of the steel slag. The working layer lining has molten steel corrosion and thermal load. The permanent layer lining has no corrosion but only thermal load. The life span of magnesium slag layer is 79 heats, and the actual

life is 40 times; the life of aluminum-magnesium carbon work layer is 136 heats, and the actual life is 80 heats; the life of high-aluminum permanent layer is 158 times, and the actual life It's about 160 heats. This shows that the calculation results of the liner life of each layer are basically the same as the actual life.

TABLE 6

Maximum thermal stress of the lining of each layer under three supporting conditions

Maximum thermal stress (MPa)		Support state		
		Lifting	On the trolley	Landing
Layers lining	Working layer (aluminum magnesium carbonaceous)	45.0	40.9	37.4
	Permanent layer (micro expansion high aluminum)	41.6	38.5	35.7
	Slag layer (magnesium carbon)	20.1	19.2	18.1

TABLE 7

Life of the individual linings of the ladle under thermomechanical stress alone

Layers lining	Experimental parameters		Life (heating times)
	A	B	
Working layer (aluminum magnesium carbonaceous)	−1.58	48	79 (Thermal mechanical stress alone)
Permanent layer (micro expansion high aluminum)	−13.20	69.8	136 (Thermal mechanical stress alone)
Slag layer (magnesium carbon)	−13.61	50.1	158 (No corrosion)

5. Conclusion

In this paper, the fatigue life of the steel cladding is calculated by using conventional fatigue combined with fracture propagation, and the predicted life is basically consistent with the service life of the steel cladding, which shows that the method used in this paper can effectively predict the life of the steel cladding. In the calculation of ladle life using the fracture propagation theory, it can be seen that the length of the initial crack can affect the service life of the steel ladle to a great extent. The simulation results can predict the service life of the steel cladding under different crack lengths, which is the basis for the effective maintenance period of the steel cladding maintenance. At the same time, according to the prediction results and related fault detection methods, it can further provide theoretical guidance and basis for the choice of maintenance program.

Because there are many factors affecting the life of the liner, it is difficult to consider all the factors. Therefore, this article only predicts the life of the ladle based on the nature of the liner. The service life of the ladle is calculated based on the thermal shock method. The calculation results show that the method used in this paper can basically predict the service life of the ladle. As the current methods for improving the service life of ladle linings are focused on finding suitable materials and the related production processes, there is less research on active maintenance. Therefore, the ladle lining life prediction mechanism can provide relevant data support for the maintenance of ladle lining.

REFERENCES

[1] V.V. Slovikovskii, A.V. Gulyaeva, Refract. Ind. Ceram. **54** (1), 4-6 (2013).

[2] V.A. Kononov, I.I. Zemskov, Refract. Ind. Ceram. **53** (3), 151-156 (2012).

[3] G.F. Li, J. Liu, G.Z. Jiang, Adv. Mech. Eng. **7** (4), 168781401 5575988 (2015).

[4] G.F. Li, J.Y. Kong, G.Z. Jiang, Int. Rev. Computers. So. **7** (1), 420-425 (2012).

[5] G.F. Li, J. Liu, H.H. Liu, J.Y. Kong, G. Zhen, W.T. Xiao, Y.K. Zhang, F.W. Cheng, Sensors. Transducers. **161** (12), 271-276 (2013).

[6] G.F. Li, Z. Liu, G.Z. Jiang, H.H. Liu, H.G, Xiong. Adv. Mech. Eng. **7** (6), 1687814015589667 (2015).

[7] S.G. Kahrizsangi, H.G. Dehsheikh, M. Boroujerdnia, Mater. Chem. Phys. **189**, 2230-236 (2017).

[8] J. Yenus, G. Brooks, M. Dunn, Metall Mater Trans B. **47** (4), 2681-2689 (2016).

[9] G.F. Li, P.X. Qu, J.Y. Kong, G.Z. Jiang, L.X. Xie, P. Gao, Z.H. Wu, Y. He, Appl. Math. Inform. Sci. **7** (3), 1043-1050 (2013).

[10] G.F. Li, P.X. Qu, J.Y. Kong, G.Z. Jiang, L.X. Xie, P. Gao, Z.H. Wu, Y. He, Appl. Math. Inform. Sci. **7** (2), 439-448 (2013).

[11] R.A.A. Borges, G.F.B.L.E. Silva, Eng. Fail. Anal. **78**, 161-168.

[12] X. Zhou, Z. Tang, G. Qu, Mat. Sci. Eng. A-Struct. **527** (9), 2327-2334 (2010).

[13] G.F. Li, W. Miao, G.Z. Jiang, Y.F. Fang, Z.J. Ju, H.H. Liu, Discrete. Cont. Dyn-S. **8** (6), 1223-1237 (2015).

[14] G.F. Li, J.Y. Kong, G.Z. Jiang, L.X. Xie, G. Zhao, Int. J. Inform. **12** (11), 4487-4494 (2012).

[15] H.G. Xiong, H.L. Fan, G.Z. Jiang, G.F. Li, Eur. J. Oper. Res. **257** (1), 13-24 (2017).

[16] H.G. Xiong, H.L. Fan, G.F. Li, G.Z. Jiang, Adv. Mech. Eng. **7** (9), 1687814015604546 (2015)

[17] D. Jiang, Z.J. Zheng, G.F. Li, Y. Sun, J.Y. Kong, G.Z. Jiang, H.G. Xiong, B.Tao, S. Xu, H.H. Liu, Z.J. Ju, Cluster. Comput. 10.1007/s10586-018-1844-5 (2018).

[18] F. Du, Y. Sun, G.F. Li, G.Z. Jiang, J.Y. Kong, D. Jiang, Z. Li, Int. J. Wireless. Mobil. **13** (4), 306-313 (2017).

[19] B. Li, Y. Sun, G.F. Li, J.Y. Kong, G.Z. Jiang, B. Tao, S.H. Xu, H.H. Liu, Cluster. Comput. **22** (Suppl. 1), 503-512 (2017).

[20] D.S. Chen, G.F. Li, Y. Sun, J.Y. Kong, G.Z. Jiang, H. Tang, Z.J. Ju, H. Yu, Sensors. **17** (2), 253 (2017).

[21] Y.J. Liao, Y. Sun, G.F. Li, J.Y. Kong, G.Z. Jiang, D. Jiang, H.B. Cai, Z.J. Ju, H. Yu, H.H. Liu, Sensors. **17** (7), 1491 (2017).

[22] W. Miao, G.F. Jiang, Y.F. Fang, Z.J. Ju, H.H. Liu, X.Y. Zhu, Int. J. Hum, Robot. **12** (02), 1550011 (2015).

[23] Y.F. Fang, H.H. Liu, G.F. Li, X.Y. Zhu, Int. J. Hum. Robot. **12** (2), 1550011 (2015).

[24] Y. Sun, C.Q. Li, G.Z. Jiang, D. Jiang, H.H. Liu, Z.G. Zheng, W.N. Shu, Mobile. Netw. Appl. **23** (4), 797-805 (2018).

[25] W. Dong, D. Yang, B.S. Zhang, Z.M. Wu, J. Eng. Mech. **144** (6), 04018039 (2018).

[26] Z. Li, G.F. Li, Y. Sun, G.Z. Jiang, J.Y. Kong, H.H. Liu, Int. J. Comput. Sci. Mat. **8** (1), 52-60 (2017).

[27] T. Stein, M. Wicke, A. Brueckner-Foit, T. Kirsten, M. Zimmermann, F. Buelbuel, H.-J. Christ, J. Mater. Res. **32** (23), 4354-4361 (2017).

[28] W. Miao, G.F. Li, Y. Sun, G.Z. Jiang, J.Y. Kong, H.H. Liu, Int. J. Wireless. Mobil. **11** (4), 348-356 (2016).

[29] D. Chen, G.F. Li, G.Z Jiang, Y.F. Fang, Z.J Ju, H.H. Liu, J. Comput. Theor. Nanos. **12** (12), 6126-6132 (2015).

[30] W. Li, Z. Luo, Z. Sun, Y. Hu, W.H. Duan, Mag. Concrete. Res. **70** (9), 459-472 (2018).

[31] T.L. Zhao, Z.Y. Liu, C.W. Du, C.D. Dai, X. G. Li, Mat. Sci. Eng. A-Struct. **708**, 181-192 (2017).

[32] D.S. Rabelo, J.D. Hobeck, D.J. Inman, R.M. Finzi Neto, V. Steffen, J. Intel. Mat. Syst. Str. **28** (20), 3152-3162 (2017).

[33] B. Richard, E. Kishta, C. Giry, F. Ragueneau, Mech. Res. Commun. **86**, 32-36 (2017).

[34] W.L. Ding, G.F. Li, Y. Sun, G.Z. Jiang, J.Y. Kong, H.H. Liu, Int. J. Comput. Sci. Mat. **8** (2), 138-145 (2017).

[35] D.S. Chen, G.F. Li, Y. Sun, G.Z. Jiang, J.Y. Kong, J.H. Li, H.H. Liu, Int. J. Wireless. Mobil. **12** (3), 305-312 (2017).

[36] R.J. Nims, K.M. Durney, A.D. Cigan, A. Dusseaux, C.T. Hung, G.A. Ateshian, Interface. Focus. **6** (1), 20150063 (2016).

[37] G.F. Li, Z. Liu, J.Y. Kong, G.Z. Jiang, W.J. Chang, B. Li, J.H. Li, J. Wuhan. U. Sci. Techno. **39** (1), 401-407 (2016).

[38] W.J. Chang, G.F. Li, J.Y. Kong, Y. Sun, G.Z. Jiang, H.H. Liu, Arch. Metall. Mater. **63** (2), 659-666 (2018).

[39] Y.H. Lu, P.L. Xiang, P. Dong, X. Zhang, J. Zeng, Eng Fail Anal. **89**, 222-241 (2018).

[40] A. Mantawy, J.C. Anderson, Soil. Dyn. Earthq. Eng. **109**, 46-57 (2018).